Pf3 coat protein forms voltage-gated ion channels in planar lipid bilayers

ARTICLE *in* BIOCHEMISTRY · FEBRUARY 1994

Impact Factor: 3.02 · DOI: 10.1021/bi00167a037 · Source: PubMed

3 AUTHORS, INCLUDING:

Michael Pawlak
University of Tuebingen
31 PUBLICATIONS **643** CITATIONS
SEE PROFILE

Andreas Kuhn
Hohenheim University
109 PUBLICATIONS **3,760** CITATIONS
SEE PROFILE

Pf3 Coat Protein Forms Voltage-Gated Ion Channels in Planar Lipid Bilayers†

Michael Pawlak,‡ Andreas Kuhn,§ and Horst Vogel*,‡

Institut de chimie physique II, Ecole Polytechnique Fédérale de Lausanne (EPFL), CH-1015 Lausanne, Switzerland, and Institut für Mikrobiologie, Universität Karlsruhe, Kaiserstrasse 12, D-7500 Karlsruhe, Germany

Received June 10, 1993; Revised Manuscript Received September 28, 1993®

ABSTRACT: The coat protein of bacteriophage Pf3 forms discrete and stable ion channels of uniform size in planar bilayers of asolectin. Its primary sequence suggests a channel formed by a bundle of transmembrane helices. Since the apparent transmembrane region only consists of strongly hydrophobic residues, it represents a new class of channel-forming proteins. The channel activity is strongly voltage-dependent. The single-channel conductance of 60 pS (at 100 mV) in 0.2 M NaCl is slightly voltage-dependent, indicating conformational changes of the pore upon variation of the transmembrane electric field. The channel is unselective which suggests that the pore is of aqueous character. For the observed conductance, a channel diameter of 3.6 Å is consistent with a tetrameric α-helix bundle, as calculated from a barrel-stave model. A pronounced dependence of the gating kinetics with increasing voltage arises from two opposing effects: an increase in the number of open channel structures, and a simultaneous, more than 3-fold decrease in the channel lifetime. Thus, a maximum activity is reached around 100 mV, a range which corresponds well with physiological membrane potentials. The channels activate only upon application of a positive voltage on the side of the membrane to which the protein had been added. The slow relaxation of the mean current upon application of sudden voltage jumps indicates a strong activation barrier in the channel gating process, which may result from the membrane translocation of the charged residues of the peptide ends. A channel-mediated import mechanism is suggested for the bacterial infection by phage DNA.

The coat protein of the filamentous bacteriophage Pf3 of *Pseudomonas aeruginosa* is a small protein composed of 44 amino acids (Rohrer & Kuhn, 1990):

$$M^{1}QSVITD^{-}VTG^{10}QLTAVQAD^{-}-$$
$$\underline{IT^{20}TIGGAIIVLA^{30}AVVLGIR}^{+}WIK^{+}\ ^{40}AQFF$$

It contains a very hydrophobic region of 18 residues (underlined) which separates an acidic amino-terminal segment from a somewhat shorter, basic carboxy-terminal end. The two doubly-charged regions compensate each other to give a net neutral molecule at pH 7. The protein is insoluble in water (above 1 μM) due to its largely hydrophobic character. It adopts a predominantly α-helical conformation in organic solution and in the lipid bilayer (Thiaudière et al., 1993).

Bacterial infection occurs by the import of phage DNA, which is (when in the phage form) enveloped by around 2500 copies of the protein. After multiplication in the cytoplasm, newly synthesized Pf3 coat protein inserts into the membrane prior to its reassembly into new phage particles. Membrane insertion of Pf3 coat protein and of the functionally related coat protein of *Escherichia coli* phage M13 (50 residues) is of considerable interest for the underlying biophysical mechanisms [see Kuhn and Troschel (1992) for a recent review]. The two proteins are similar in length and do not share any sequence similarity (Luiten et al., 1985). Yet, they both contain a hydrophobic region of about 20 amino acids flanked by an acidic N-terminal end and a basic C-terminal end. The acidic regions of both proteins are located in the periplasm, whereas the basic regions remain in the cytoplasm. The membrane translocation of such small proteins occurs in the presence of a transmembrane electrical potential (Gallusser & Kuhn, 1990; Kuhn, 1987; Kuhn et al., 1986) and has been shown to be independent of other proteinaceous transport components (the SecA, SecB, and SecY proteins in *Escherichia coli*) (Rohrer & Kuhn, 1990; Kuhn et al., 1990; Wolfe et al., 1985). The insertion processes of the two proteins, however, differ markedly. The primary sequence of Pf3 coat protein enables the molecule to insert spontaneously, whereas M13 coat protein needs the help of an additional 23-residue leader sequence at its N-terminus (Rohrer & Kuhn, 1990). M13 coat protein has an increased number of charged residues, five (four acidic, one basic) in the acidic segment (two acidic for Pf3 coat protein) and four basic residues (two basic for Pf3 coat protein) in the C-terminal segment. "Spontaneous" membrane incorporation is limited to the translocation of short and only weakly charged sequences. Highly charged regions can only be translocated by the cooperative action of two (or more) membrane-spanning regions in a close neighborhood, as demonstrated for the M13 procoat protein (Kuhn & Troschel, 1992).

Our interest has concentrated on the voltage-dependent insertion process of the Pf3 coat protein. We had intended to perform conductance measurements on planar lipid bilayers to follow the movement of charged residues across the membrane under the influence of voltage: interestingly, an appropriate reconstitution technique resulted in the unexpected formation of well-defined single channels.

We will present a first characterization of the voltage-dependent channel activity induced by Pf3 coat protein and explain the results in terms of a channel model. We have profited from a new, efficient purification method and a recent structure determination of the protein in organic and membrane environments (Thiaudière et al., 1993).

MATERIALS AND METHODS

Chemicals. For bilayer formation, soybean lipid (asolectin) from Sigma (Switzerland) was used and purified according

† This work was supported by grants from the European Community (Science Plan, SCCX CT 90-0025) and the Swiss National Science Foundation (FN 31-27910.89) and by the Fonds de Recherche UNIL-EPFL.

* Correspondence should be addressed to this author.
‡ Ecole Polytechnique Fédérale de Lausanne.
§ Universität Karlsruhe.

® Abstract published in *Advance ACS Abstracts,* December 15, 1993.

0006-2960/94/0433-283$04.50/0

to Kagawa and Racker (1971). 2-Propanol (p.a.), acetone (p.a.), and hexadecane (for gas chromatography) were from Merck (Germany); hexane (for UV spectroscopy) and all salts (grade microselect) were from Fluka (Switzerland). Unless otherwise stated, the buffer employed was 0.2 M NaCl/10 mM Tris-HCl, pH 7.4, prepared from pyrogen-free water (18 MΩ·cm) of a Barnstead Nanopure system and passed through 0.22-μm Millex GS filters before use.

Isolation of Pf3 Coat Protein. Pf3 phages were grown by infection of *Pseudomonas aeruginosa* and stored as a stable suspension in 0.1 M Tris-HCl (pH 7)/0.1% NaN_3 at 4 °C. For the experiments, the Pf3 coat protein was freshly extracted with 2-propanol/0.1% TFA from aliquots of the phage suspension. Protein purification and analysis are described in detail elsewhere (Thiaudière et al., 1993). For the experiments, 15 μM stock solutions of the protein were prepared in 2-propanol/0.1% TFA and stored at −20 °C. HPLC analysis on a Nucleosyl 100-7 C2 reverse-phase column revealed a major peak with more than 90% purity (minor peaks could be attributed to aggregated protein). The protein stock solution lost around half of its pore-forming capability after 4 months of storage at −20 °C.

Planar Bilayers and Current Measurements. The setup and the procedure for the electrical measurements have been described previously (Pawlak et al., 1991). Planar lipid bilayers were formed according to the method described by Montal and Mueller (1972) across a hole of 100-μm diameter in a Teflon septum, separating two compartments of 2-mL volume each. The hole was pretreated with a small amount of a 1:40 hexadecane/hexane solution. The bilayer was folded from two monolayers which had been spread at the air/water interface after addition of 10 μL of a 5 mg/mL lipid/hexane solution to each side and allowing the organic solvent to evaporate for 3 min. Membrane formation was followed by the increase in capacitance on applying a triangular voltage (50 Hz, ±10 mV). The aqueous compartments were connected to the measuring circuit via Teflon-isolated Ag/AgCl electrodes. Currents were measured with a BLM-120 amplifier (Biologic, France), using a headstage with a 10^{10}-Ω feedback resistance, directly linked to the electrodes. Individual voltage sequences could be applied to the membrane from a programmable stimulator (SMP-310, Biologic). Data analysis was performed using the program Biopatch (Biologic).

The protein was added from the stock solution to one side of the membrane (cis). Either the trans or the cis electrode could be activated as the working electrode, the counter-electrode always being grounded. The sign of the applied voltage refers to the active side. Routinely, the side of protein addition was grounded. Thus, application of negative potentials resulted in negative current signals (see Figures). Experiments were conducted at room temperature (22–25 °C).

The electrical conductivities of the electrolytes were determined with a Philips PW 9505 conductivity meter: 20 mS/cm for 0.2 M NaCl, 23 mS/cm for 0.2 M KCl, and 23 mS/cm for 0.2 M CsCl. All solutions were buffered with 10 mM Tris-HCl, pH 7.4; the buffer contributed a maximum of 5% to the total conductivity.

Electronic Recording and Data Processing. Depending on the lifetimes of the channels, the current signals were filtered at 300 Hz (for voltages $V \leq 130$ mV) and at 1 kHz ($V > 130$ mV), by means of a built-in 5-pole Tchebicheff filter. The output signals were recorded on a digital tape recorder (DTR-1200, Biologic) and simultaneously observed on a digital storage oscilloscope (2221A, Tektronix). For further evaluation, the records were transferred to the hard disk of a PC (486/33 MHz) with a sampling period of 1.7 ms ($V \leq 130$ mV) and 0.5 ms ($V > 130$ mV) per point. If necessary, the data were further filtered by software (using a Hanning window), at the frequency which indicated the transition into white (electronic) noise [estimated from the power spectral density (Sakman & Neher, 1983)]. Single-channel conductances were calculated from current histograms best-fitted by the sum of multiple Gaussian distributions, using continuous recordings of 1–2-min duration. The current recordings were characterized by n, the total number of events (in all current levels, $k = 0, 1, 2, 3, \ldots$), p_k, the state probabilities, i.e., the times where the current remained in level k during the observation period, and N, the number of channels generating the current signals (with multiple openings). m denotes the number of experiments on different membranes.

RESULTS

Reconstitution of Single Channels. Initial experiments were performed by adding small amounts of the protein stock solution, while stirring, to the buffer close to the bilayer (cis). No increase of membrane conductance could be observed when a constant voltage of up to ±200 mV was applied, except for rather short-lived current spikes, which appeared as positive and negative deviations from the bare membrane signal at one polarity of the applied voltage. The situation did not change even for 1 h after protein addition. However, when by chance the membrane broke and was re-formed by lowering and reraising the water level of the cis side, discrete, channellike current steps, i.e., sharp transitions between constant current levels, could be observed (similar to those shown in Figure 1). After having made this observation, we changed our experimental routine as follows: after spreading the lipid monolayers, we applied 1 μL of the 15 μM protein solution (2-propanol/0.1% TFA) to the top of the air/water interface of the cis side and stirred subsequently for 30 s. We waited for about 10 min, to allow the organic solvent to evaporate and/or dissolve into the aqueous solution, and then formed the bilayer by raising first the trans and then the cis level of the electrolyte over the hole. After waiting another 10–30 min, we started the electrical measurements. Single-channel currents, as described above, could now be reproducibly observed, in a defined system, with the trans side never having been directly exposed to the protein ($m = 18$) (see Figure 1). The channel activity established voltage-dependent and was always fully asymmetric; i.e., current steps appeared only when a negative voltage was applied to the trans side of the membrane. The current traces were stable upon application of constant voltages for several minutes. The channel characteristics—the amplitudes of the current steps and the asymmetry of the channel activity—were comparable to the measurements which were performed on the re-formed bilayers. No changes of the characteristics could be observed when the measuring electrode was set active on cis instead of trans (except that channels with positive current amplitudes were now activated by positive voltages) or when the protein was added from the trans side. As a control, comparable amounts (~1 μL) of a 2-propanol/0.1% TFA solution, containing no protein, were added to the lipid monolayer using the same routine. The stability of the bilayers was not affected by these amounts of organic solvent, and no transitions of the bare membrane conductance into higher levels could be observed.

Voltage-Dependent Channel Characteristics. Figure 1 shows the voltage-dependent characteristics of Pf3 coat

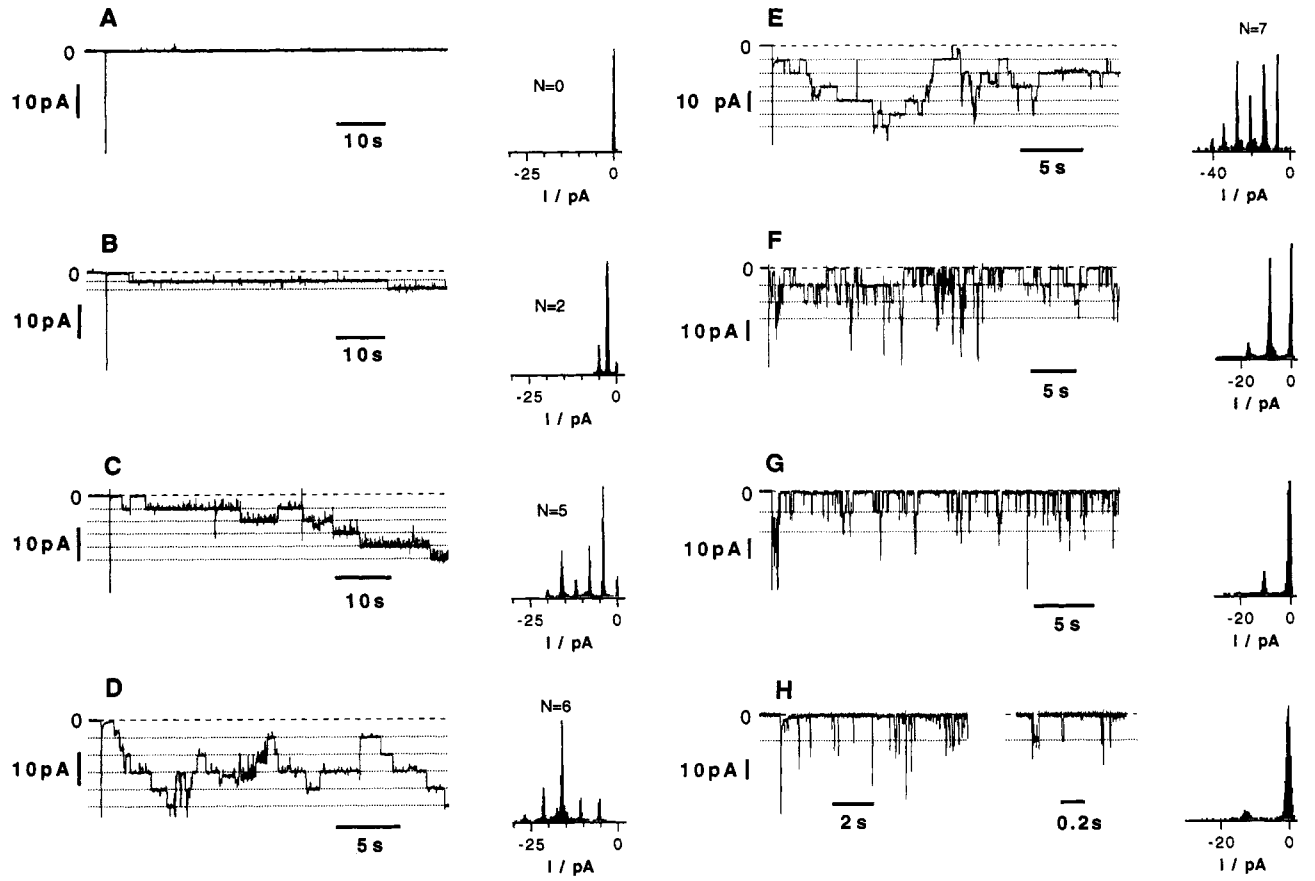

FIGURE 1: Voltage-dependent channel activity of Pf3 coat protein reconstituted in asolectin bilayers from the cis side (0.2 M NaCl/10 mM Tris, pH 7.4). Left side: first sections of current recordings (1–2 min) after sudden application of a constant negative voltage, V (trans) (indicated by the capacitance spike): (A) 30 mV; (B) 50 mV; (C) 70 mV; (D) 90 mV; (E) 110 mV; (F) 130 mV; (G) 150 mV; (H) 170 mV [filter frequencies were 300 Hz (V = 30–130 mV) and 500 Hz (V = 150–170 mV)]. The dashed lines and the dotted lines indicate zero current and equidistant current levels $k = 1, 2, 3, \ldots$, respectively. Right side: current histograms of the recordings (frequency of occurrence in arbitrary units) and number of channels N obtained by fitting the experimental distributions of the respective levels k to binomial distributions. The current histogram (panel H) is shown for the trace section with the better time resolution.

protein-induced channel activity at a series of different voltages (negative trans). Constant voltage steps of a duration of around 2 min were applied to the membrane, starting at low voltages and increasing in steps of 10 mV (in the following, we use the term voltage irrespective of its sign). Current signals appeared with comparable characteristics after repetitive application of the same voltage. Single-channel currents were in the range 1–10 pA. The amplitude histograms, shown on the right-hand side of Figure 1, demonstrate the voltage-dependent occurrence of multiple openings into equidistant levels, k, indicating the simultaneous activation of many channels, N. The maximum level number, k_{max}, in the different experiments was rarely reproducible (k_{max} = 1–8). For the presentation of Figure 1, the first sections of the current records, where the voltage was switched from zero to the particular voltage (indicated by the capacitive spike of the membrane), were chosen to note the voltage-dependent activation.

For all records, we evaluated the distribution of the state probabilities p_k of the individual levels k using the normalized areas under the multiple Gaussian functions. For two experiments, revealing comparable large level numbers (k_{max} = 7, 8 at 100 mV), Figure 2 shows the voltage-dependent channel activity over the whole range of voltage in terms of $1-p_0$, the probability of being not in the closed state. Clearly, a critical voltage is necessary to establish channel formation. No activity could be observed over a period of minutes for voltages below 40 mV (see Figure 1A). When the voltage

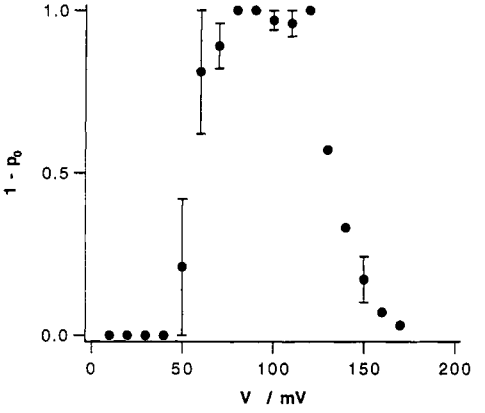

FIGURE 2: Voltage-dependent channel activity expressed in terms of $1-p_0$, the probability of not being in the closed state (two experiments with comparable maximum multiple levels k_{max} = 7, 8 at 100 mV). The values of p_0 were taken from Gaussian fits to current histograms of recordings lasting 1–2 min ($n \geq 30$ at V = 50–70 mV, $n \geq 500$ at V = 80–100 mV, $n \geq 1000$ for V = 100–150 mV, $n \geq 300$ at V = 160, 170 mV). Error bars indicate mean deviations from different experiments.

was raised to 50 mV, stable and long-lasting open states (≥10–60 s) appeared after some time lag (Figure 1B). Application of higher voltages reduced this time lag and increased the probability of channel formation (Figure 1C,D,E). Simultaneously, the lifetime of the channels decreased to a few seconds. At 110 mV, pores opened instantaneously (Figure 1E). A maximum activity was reached around 100 mV (Figure

2). At higher voltages, the channel lifetimes strongly shortened into the range of ≤10 ms (at 170 mV) (Figure 1F,G,H). In summary, the strong voltage-dependence of the channel activity induced by Pf3 coat protein can be explained by two compensating effects upon increasing the voltage: an enhanced activation of open channel structures and an apparent inactivation due to a pronounced reduction of channel lifetimes, resulting in a maximum activity at around 100 mV.[1]

It should be noted that sublevels of lower conductance appeared in a minor fraction of the transitions. Especially when a long-lasting pore opened, sporadic bursts of rather fast transitions (in the millisecond range) to a partially, but not fully closed level occurred (see Figure 1C). We did not include these levels in the evaluation, because channel activity was dominated by the long-lasting states.

Current–Voltage Relationship. Two methods were used to evaluate the current amplitudes of the discrete levels at different voltages. First, a statistical analysis was performed using large numbers of events. The single-channel currents were evaluated from Gaussian fits of the amplitude histograms of the records, including single- and multiple-level experiments. The black dots in Figure 3A show the current–voltage characteristics of the channels from this analysis. Due to the low activation rate of channels at low voltages, the current amplitudes between 0 and 50 mV were obtained by waiting for a long open state at 50 mV and then successively switching the voltage back to zero in steps of 10 mV (n = 18, m = 3). A different technique was employed, taking advantage of channel lifetimes in the time range of seconds: once a pore with a long lifetime was activated (at 50–60 mV), some cycles of a triangular wave (1 Hz, ±100 mV) were applied on top of the constant holding potential (Figure 3B). In such a way, complete I–V curves of individual single channels between +50 and −150 mV were available within a short time period. Since the speed of the voltage ramps was high compared to the channel lifetime, the pore could not relax instantaneously and remained open, even when the applied voltage switched to a positive sign. However, in most cases the pore closed after the first half-cycle when the voltage reached +50 mV (see Figure 3B). Thus, the voltage dependence of the bare membrane (with no channel being open) was simultaneously measured in the following cycles. After correction for the capacitive and the bare membrane current, continuous I–V curves of the individual single channels were obtained, including extensions into the branch of positive voltages (solid line in Figure 3A). The current–voltage curves of different individual channels were reproducibly superimposable to the I–V curve obtained from the statistical analysis, as shown in Figure 3A (n = 15, m = 3).

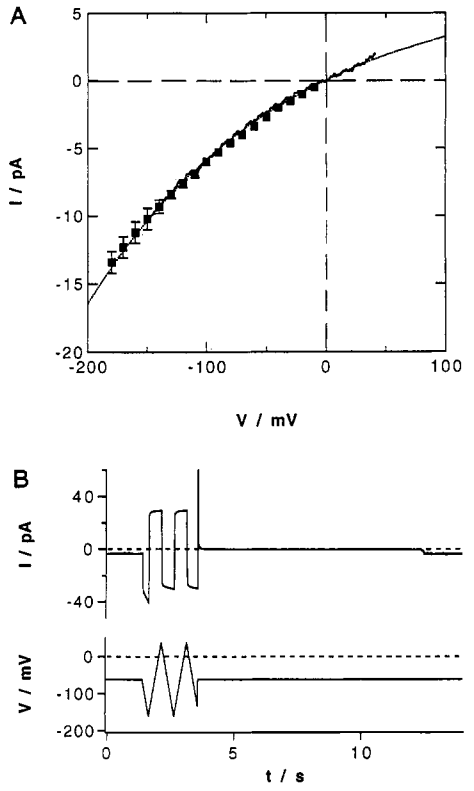

FIGURE 3: (A) Current–voltage characteristics of Pf3 coat protein single channels. Solid symbols represent the results of a statistical analysis based on a large number of openings [n = 18 at 0–40 mV (m = 3), n > 100 at 50–70 mV and n > 1000 at 80–120 mV (m = 13), n > 2000 at 130–150 mV (m = 3), n > 300 at 160, 170 mV (m = 3), $n \geq 50$ at 180 mV (m = 2)]. The continuous curve shows one of several experiments revealing the I–V curves of individual single channels (n = 15, m = 3) according to the protocol shown in (B) and described in the text. The dotted line is a monoexponential fit of $I = I'[1 - \exp(-V/V_{IV})]$ with I' = 7.1 pA and V_{IV} = 167 mV. Error bars indicate mean deviations from different experiments, including standard deviations of the Gaussian functions of multiple openings. (B) Single-channel cyclic voltammogram: some cycles of a triangular voltage (±100 mV, period 1 s) (bottom) were applied to an open channel (top trace) which had been activated by a constant holding potential of −60 mV (see beginning of current trace). The channel closed during the applied cycles and opened again after some seconds (at the end of the trace).

The current–voltage characteristics revealed a perceptible, although slight, voltage dependence: the single-channel currents increased more strongly than linearly with voltage. It could be fitted by a monoexponential function, $I \sim 1 - \exp(V/V_{IV})$, with a characteristic, e-fold increase every V_{IV} = 160 ± 20 mV (see dotted line in Figure 3A). The single-channel conductances were 54 ± 4 pS (50 mV), 60 ± 2 pS (100 mV), and 68 ± 6 pS (150 mV). The voltage dependence demonstrates that variation of the transmembrane electric field is also able to slightly affect the size of the channel.

Time Relaxation after Sudden Voltage Change. We investigated how fast channel activity could arise after a sudden voltage jump. To achieve a good statistical significance, a larger number of channels should contribute to the current response. We recorded 15 successive single-channel traces, applying repetitive voltage pulses from zero to a constant value (120 mV) (m = 2). The pulse duration and the time between

[1] The state probabilities, p_k, could be well described by binomial distributions at voltages up to 120 mV, thus revealing the number of independent channels, N, which contribute to the signals. These numbers N corresponded well to the maximum multiple levels, k_{max}, detected in the records (N values, determined for the respective traces, are shown in the amplitude histograms of Figure 1). With increasing voltages, larger N than k_{max} could always better adjust the distribution of the experimental-state probabilities, and in spite of reduced channel lifetimes, the number of openings per second did not diminish. In fact, it turned out, that for $V \geq 130$ mV ($n \geq 1000$ for 130–160 mV, $n \geq 500$ for 160–170 mV), the Poisson distribution (as the binomial limit for high N and a low open probability of an individual channel, p_{open}) fitted well, using the average $\langle k \rangle = \sum k p_k = N p_{open}$ as a parameter. Apparently, N is permanently increased with higher voltages. However, application of Poisson statistics means that direct information about the number of channels N and p_{open} is then lost because of the product. Generally, our measurements were dominated by multichannel traces, and sections of single openings of sufficient length, necessary for the evaluation of a many-channel system (Jackson, 1985), were not attainable for a good determination of the channel lifetime and the open probability p_{open}. Nevertheless, we can estimate from the experimental data a strong, more than 3-fold reduction of the mean channel lifetime with increasing voltage. Thereby, the values at the higher voltages have a good significance. At 140–170 mV, $1 - p_0$ in Figure 2 practically corresponds to p_{open}, because the records included more and more single-channel sections. From that point of view, the Poisson statistics seem to be justified.

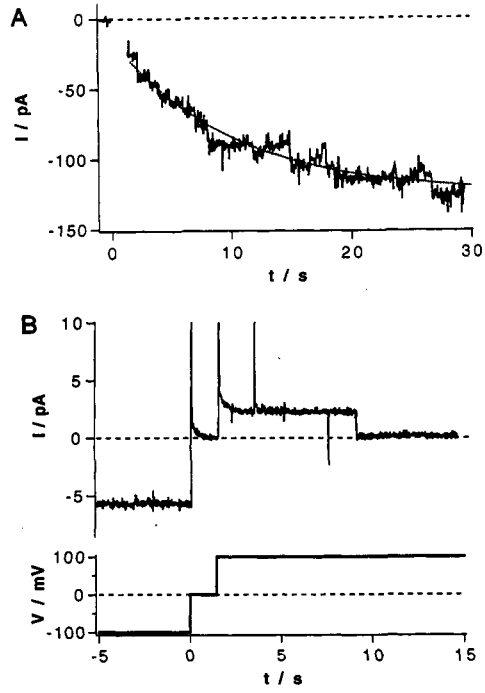

FIGURE 4: (A) Current relaxation of Pf3 coat protein channels into the new stationary state after application of a voltage jump from 0 to −120 mV (at time zero). The current response is a superposition of 15 individual single-channel recordings upon repetitive application of voltage pulses of 60-s duration ($n \geq 100$, $m = 2$). The capacitance spike has been removed. The dotted line is a monoexponential fit with a characteristic time constant of $\tau = 10$ s. (B) Typical current response of Pf3 coat single channels upon changing the polarity of the holding potential from transnegative to transpositive: −100 mV|0 mV|+100 mV ($n = 23$, $m = 5$).

two pulses was 60 s in every case. The individual current traces were superimposed on the computer [cf. p 143 of Sakman and Neher (1983)]. The result is presented in Figure 4A. The activity revealed a clear relaxation from zero current to a final stationary state. The time course was of first order and could be well fitted by a single-exponential function having a characteristic relaxation time $\tau = 10 \pm 2$ s (dotted line in Figure 4A).

In another type of experiment, we concentrated on the relaxation when, in an open state, the voltage was switched from a particular value to zero and then to the same value of opposite sign. The channel current instantly fell to the signal of the bare membrane at zero voltage. The moment the voltage changed to the value of opposite sign, a smaller current amplitude appeared instantly (Figure 4B). This indicates that the pore structure was still present even without applied voltage. After a short period of time, the open state disappeared, and the channel remained in the closed state. The reduced current amplitude is evident if one follows the voltage-dependent I–V curve into its positive voltage branch, where the amplitudes are smaller compared to those at negative values. Each time the voltage was switched between negative and positive values, the respective currents corresponded to the values of the I–V curve in Figure 3A ($n = 23$, $m = 5$). This behavior further supports the existence of a voltage-dependent current–voltage curve. Clearly, the channel structure remains stable even in the absence of voltage. Voltage of opposite sign is likely to accelerate the closing of the channel.

Concentration Dependence and Ion Selectivity. For the reconstitution method described, the number of channels that could be opened simultaneously (corresponding to k_{max} at 100 mV, see above) varied roughly between 1 and 10 in the different experiments and could hardly be controlled. Addition of less protein to the monolayer at the beginning produced almost no activation, whereas higher concentrations increased the probability of membrane rupture (see also Discussion). Therefore, we were restricted to a small concentration range, and determination of the concentration-dependent channel activity was not feasible.

The ionic selectivity of Pf3 coat channels was determined by measuring the reversal potentials of the I–V curve after establishing a concentration gradient of NaCl across the bilayer [0.1 M (cis), 0.6 M (trans)]. No notable shift of the I–V curve could be observed ($m = 3$). This suggests that the channels formed by the Pf3 coat are rather unselective in conducting ions and of aqueous character. The observation was corroborated by measurements in symmetrical 0.2 M KCl ($m = 2$), where the current–voltage curve shifted to 10% higher current values according to the slightly enhanced specific bulk conductivity of KCl over NaCl. However, at 0.2 M CsCl, the single-channel currents decreased by a factor 0.65 compared to NaCl ($m = 2$), although the specific conductivity reaches that of KCl. We attribute this to a reduced conductivity of the larger Cs^+ ions inside the channel.

DISCUSSION

We have discovered that the coat protein of bacteriophage Pf3 is capable of forming discrete ion channels in planar lipid bilayers, even though its amino acid sequence cannot adopt a membrane-spanning amphiphilic structure. Amphiphilic α-helices or β-structures are thought to be necessary for channel formation according to a barrel-stave model [see Sansom (1991) for a recent review]. Pf3 coat protein channels were reconstituted from a homogeneous and structurally defined protein sample (Thiaudière et al., 1993) into an artificial lipid bilayer system. The planar membrane was prepared from asolectin, a mixture of soybean lipids including negatively charged lipids, which has been shown to form stable bilayers for the functional reconstitution of protein channels as large as the ligand-gated acetylcholine receptor (Schindler & Quast, 1980; Montal et al., 1984). Appropriate addition of Pf3 coat protein to one monolayer induces the opening of rather stable and long-lasting ion channels some minutes after folding the bilayer. The channels had uniform conductances, and could only be activated by application of one polarity of the membrane potential. The channel activity is strongly voltage-dependent. The mechanism of channel formation *per se* is one aspect of interest and will be discussed in relation to other small, but amphiphilic, peptides which exhibit channel-forming activity, like alamethicin (20 residues, hydrophobic, singly negatively charged or uncharged) (Boheim et al., 1983) and melittin (26 residues, highly positively charged) (Tosteson & Tosteson, 1981; Pawlak et al., 1991). Another aspect addresses the mechanism of protein insertion and translocation across the bacterial membrane and its regulation by the membrane potential. We propose the following mechanisms for the interpretation of our results.

Protein–Bilayer Interaction. A sufficiently strong protein–membrane association is required for the observation of channel activity. Pf3 coat protein has a pronounced hydrophobic character. It adopts a mainly α-helical conformation with an average helix content of 90% in organic stock solution and 40% in aqueous environment, as judged by circular dichroism (Thiaudière et al., 1993). It shows a strong affinity for lipids. In aqueous solution (1 mM Tris-HCl, pH 7.4), the protein strongly aggregates, forming oligomers of up to 10 monomers

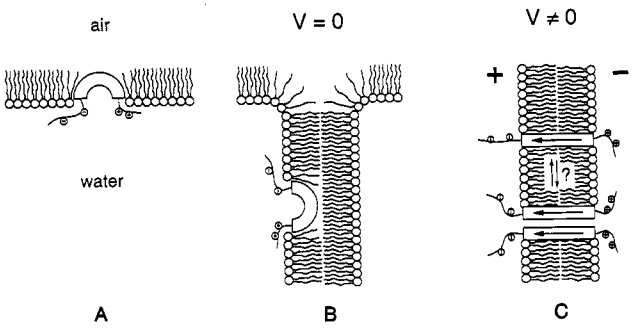

FIGURE 5: Tentative model for Pf3 coat protein/bilayer interaction and ion channel formation: (A) protein associates with the monolayer formed at the air/water interface; (B) two monolayers fold into a bilayer with protein inserted only on one side of the membrane (in the absence of an electric field); (C) application of an electric field forces the protein into a transmembrane orientation (the C-terminal end translocation shown). The arrow indicates the direction of the dipole moment (separation of half an elementary charge over the distance of the membrane thickness) generated by the α-helical segment of the protein (box). Only a transnegative voltage results in channel activity.

at a concentration of 1 μM. After some hours, it even starts to precipitate (E. Thiaudière, unpublished results). The hydrophobic character of the protein forced us to add small amounts from a defined stock of organic solution, where the molecules comprise a monomeric state. When the protein was added directly to the 200 mM salt solution, we attribute the lack of channel activity to a strong self-aggregation in water and/or to a strong adsorption to the Teflon walls, which drastically lowers the pool of membrane active molecules. The number of increased deviations from the bare membrane current (see Results), however, suggests that at least some protein interacted with the membrane. This might be due to the association of aggregated forms which cannot be transformed into channel-forming structures. In contrast, direct protein addition on top of the monolayer allows an immediate and good contact with the hydrophobic environment of the lipids (Figure 5A). We surmise that the very hydrophobic stretch of the protein (positions 19–36) is embedded in the hydrocarbon region of the monolayer, anchored electrostatically by the basic residues of the C-terminal end. By folding the two monolayers, a bilayer with coat protein preferentially associated in a monomeric state on one side of the membrane may then be formed in the absence of an electric field (Figure 5B). According to the spectroscopic investigations, the protein adopts a structure between 50% and 70% α-helix content in the lipid bilayer, depending on increasing amounts of negatively charged lipids (Thiaudière et al., 1993). In this configuration, the α-helix could correspond to the length of the membrane-embedded hydrophobic stretch and the basic C-terminal end. On the basis of the amounts of protein added in the experiments, we can estimate an upper limit of the lipid to protein ratio of 5000 in one half-bilayer. The actual ratio, however, might be much less due to loss of protein into the aqueous solution during addition to the lipid monolayer. This might also explain the varying number of multiple levels in the different experiments. Under these circumstances, the amount of protein which participates in channel formation comprises only a minor fraction of the membrane-associated molecules. The bulk of membrane-associated protein, not involved in the channel formation process may destabilize the bilayer at high transmembrane voltages (see Figure 1H) and explain an enhanced probability for membrane rupture upon addition of a higher protein dose. A similar effect is reported for small channel-forming peptides (Stankowski et al., 1991).

Voltage-Dependent Protein Insertion. A second important step is the transformation of membrane-associated protein into a channel-forming complex with at least a part of the protein in a transmembrane orientation. Such a complex might be formed by spontaneous monomer aggregation into an almost fixed number of closed-channel structures, which would open upon voltage-dependent, internal changes of conformation, or only a transmembrane potential of proper sign would allow for the transmembrane configuration of surface-associated protein monomers, which then aggregate statistically. Having our experimental results in mind [e.g., an increasing, low number of open channels formed by a large bulk of latent, closed-channel structures (Poisson statistics), slow relaxation of the channel activity, the need for a critical field strength, and strongly conserved activation upon one-voltage polarity], we interpret the process of channel gating predominantly in terms of voltage-dependent protein insertion across the membrane, in relation to the biochemical studies (Kuhn & Troschel, 1992). By analogy, the voltage-dependent channel activity of small, amphipathic peptides is generally explained as voltage-dependent membrane insertion of the molecules [see Sansom (1991, 1993)].

An α-helix composed of 20 amino acids in the hydrophobic segment of Pf3 coat protein (positions 18–37) would be sufficient to span the ca. 30-Å-thick hydrophobic region of the asolectin bilayer. In this conformation, the molecule generates a strong permanent electrical dipole moment (i) due to the unidirectional orientation of peptide bonds of the α-helix backbone [20 residues correspond to around 68 D, equivalent to a partial charge separation of $+^1/_2$ at the N-terminal end and $-^1/_2$ at the C-terminal end (Hol et al., 1981)] and (ii) due to the separation of the 2 positively and 2 negatively charged residues [the separation of 1 positive and 1 negative charge over a distance of 30 Å would be equivalent to a dipole of 150 D, oppositely directed to (i)]. Thus, we assume that the main action of the applied voltage is to orient the surface-associated protein (or parts of it) along the electric field (Figure 5C). However, it remains to be clarified whether the charged residues and/or the α-helical dipole moment dominate as a voltage sensor. Subsequent channel formation could result from aggregation of membrane-spanning monomers. The slow relaxation upon a voltage jump (Figure 4A) indicates a strong activation barrier which could be accounted for by the movement of the charged residues across the membrane. The height of the energy barrier will also depend on the protonation state of these residues. In addition, the membrane-spanning part could be stabilized in its position by the charged residues, as shown for synthetic peptides (Roux et al., 1989; Nezil & Bloom, 1992). This might explain the long lifetimes of the channels. Once an open channel is in the transmembrane configuration, it evidently takes some time to inactivate. This process can be accelerated by application of the inverse potential, as demonstrated experimentally (Figure 4B). However, when no channel structure was present (after a longer relaxation at zero voltage), no channel could be activated at transpositive potentials. A critical voltage seems to be necessary to obtain an observable open-state probability. Increasing voltage promotes the number of open-channel structures, apparently by orienting more and more associated protein as considered for the voltage-dependent channel gating of the small and flexible peptide alamethicin (Baumann & Mueller, 1974; Fox & Richards, 1982). However, a second competing process must occur, which decreases the channel lifetime in a strongly voltage-dependent manner. The electric field is obviously

involved in further conformational changes of the channel aggregate, indicated by the voltage-dependent I–V curve (Figure 3A): stronger fields may tend to push the α-helices out of the membrane. Less stabilized aggregates with shorter lifetimes and bundles of varying size could result. A voltage-dependent channel lifetime has also been observed for the highly charged channel peptide melittin (Pawlak et al., 1991) in contrast to the uncharged peptide alamethicin. The strong voltage dependence of the channel gating could be attributed to the translocation of maximal 1.5 charges and/or dipole contributions across the full or only part of the membrane thickness. The transport of charged residues across the hydrophobic barrier, necessary for channel formation, has already been reported in the case of melittin (Tosteson & Tosteson, 1981; Pawlak et al., 1991). The two opposed mechanisms would provide a minimum channel activity around 100 mV, a value which corresponds well to physiological membrane potentials. Both voltage-dependent activation and voltage-dependent inactivation are features which resemble the characteristics of channels formed by large protein moieties (Hille, 1984); they have not yet been observed simultaneously for small channel-forming peptides.

Single-Channel Formation. Pf3 coat protein forms single channels with a uniform conductance of 60 pS at 100 mV. Using this value and the bulk conductivity of our buffer solution, we calculate a channel diameter of 3.6 Å. According to a barrel-stave model, this radius would correspond to a transmembrane bundle of four α-helices of 10-Å diameter [see Sansom (1991) for the calculation]. Presumably due to its primary sequence, the protein only appears capable of stabilizing in one distinct ion-conducting aggregate. This is in contrast to the broad distribution of channel structures of the pore-forming, amphiphilic peptides (Sansom, 1991); the conductance of 60 pS is comparable to that of their low aggregation states. The strong rectification upon voltage polarity is indicative of the parallel alignment of protein monomers within the channel aggregate. Pf3 coat channels turned out to be rather unselective, actually simulating a water-filled membrane pore. This is comparable to the more or less hydrophobic alamethicin channel, which showed only weak cation selectivity, which decreases upon increasing channel size (Gordon & Haydon, 1975; Hall et al., 1984). In line with the idea of a water-filled pore structure is the observation of a slightly enhanced channel conductance of KCl over NaCl according to the increased specific bulk conductivity. The channel current in CsCl, however, is lowered by a factor 0.65. We attribute this to the finite size of the Cs^+ ions. A hydrodynamic diameter of 3.4 Å is taken from Hille (1984). This is close to the calculated pore diameter of 3.6 Å. Thus, a reduced mobility of the Cs^+ ions within the channels could be explained by "frictional" effects due to structurally modified hydration of the ion near the proteineaceous pore wall.

Biological Relevance of Channel Formation. Given the strong lytic and antibacterial activity of melittin, the Pf3 coat protein channels of comparable size should be toxic to the bacterium after massive protein insertion from the cytoplasm. The membrane potential, however, is directed such that positive polarity is at the periplasmic side (Rohrer & Kuhn, 1990). Thus, channel formation might only develop when protein associates from the outside. A possible function of the channel may be to support the import of phage DNA across the bacterial membrane. The phage particle, once coupled to the plasma membrane, could release high local concentrations of coat protein. The negative potential on the cytoplasmic side would force the protein to translocate. A high local protein concentration favors the aggregation process. The associated DNA could then be imported by a channel-mediated process. During translocation of the DNA, the channel would be at least partially blocked. This might prevent the exchange of vital cell fluids and an osmotic imbalance. Subsequently, the channels might dissociate by lowering of the local protein concentration due to lateral diffusion into less concentrated regions of the plasma membrane. In addition, local deviations from physiological membrane potential might help to inactivate the channels. One should note that newly synthesized Pf3 coat protein in the cytoplasm inserts uniformly oriented into the plasma membrane under the influence of the membrane potential (Rohrer & Kuhn, 1990) but is not able to assume an open channel structure. A similar channel mechanism, regulated by signal peptides, was recently proposed for the process of protein translocation across the membrane (Simon & Blobel, 1992).

CONCLUSION

We have shown that Pf3 coat protein can be inserted into lipid bilayers in a transmembrane configuration upon application of an electric field. The membrane-associated form represents a new class of small channel-forming proteins, which are hydrophobic and, with around 50 residues, twice as large as the classical, small pore-forming peptides, which are just able to span the bilayer thickness. Pf3 coat protein already shows some features of large protein channels, such as voltage-induced inactivation. Because ion channel formation represents a good tool to study the voltage-dependent mechanism of protein insertion, it may reveal new aspects on the function of signal peptides and their importance to protein translocation across the membrane. We are on the way of performing further experiments with Pf3 coat analogs, genetically modified especially in the charged regions of the protein. This is to define the specificity of the protein insertion process in the presence of transmembrane electric fields and to gain more information on the voltage-dependent structure and function of the protein in membranes.

ACKNOWLEDGMENT

We are grateful to Dr. D. Engelman, Dr. M. Liley, and Dr. D. Fraser for critical reading of the manuscript and to M. Soekarjo for isolating the Pf3 coat protein.

REFERENCES

Baumann, G., & Mueller, P. (1974) *J. Supramol. Struct. 2*, 538–557.

Boheim, G., Hanke, W., & Jung, G. (1983) *Biophys. Struct. Mech. 9*, 181–191.

Fox, R. O., & Richards, F. M. (1982) *Nature 300*, 325–330.

Gallusser, A., & Kuhn, A. (1990) *EMBO J. 9*, 2723–2729.

Gordon, L. G. M., & Haydon, D. A. (1975) *Philos. Trans. R. Soc. London, B 270*, 433–447.

Hall, J. E., Voydyanoy, I., Balasubramanian, T. M., & Marshall, G. R. (1984) *Biophys. J. 45*, 233–247.

Hille, B. (1984) *Ionic Channels in Excitable Membranes*, Sinauer Associates, Sunderland, MA.

Hol, W. G. J., Halie, L. M., & Sander, Ch. (1981) *Nature 294*, 532–536.

Jackson, M. B. (1985) *Biophys. J. 47*, 129–137.

Kagawa, Y., & Racker, E. (1971) *J. Biol. Chem. 246*, 5477–5487.

Kuhn, A. (1987) *Science 238*, 1413–1415.

Kuhn, A., & Troschel, D. (1992) in *Membrane Biogenesis and Protein Targeting* (Neupert, W., & Lill, R., Eds) pp 33–47, Elsevier, New York.

Kuhn, A., Wickner, W., & Kreil, G. (1986) *Nature 322*, 335–339.

Kuhn, A., Zhu, H.-Y., & Dalbey, R. E. (1990) *EMBO J. 9*, 2385–2388.

Luiten, R. G. M., Puttermann, D. G., Schoenmakers, J. G. G., Konnings, R. N. H., & Day, R. L. (1985) *J. Virol. 56*, 268–276.

Montal, M., & Mueller, P. (1972) *Proc. Natl. Acad. Sci. U.S.A. 69*, 3561–3566.

Montal, M., Labarca, P., Fredkin, D. R., & Suarez-Isla, B. A. (1984) *Biophys. J.*, 165–174.

Nezil, F. A., & Bloom, M. (1992) *Biophys. J. 61*, 1176–1183.

Pawlak, M., Stankowski, S., & Schwarz, G. (1991) *Biochim. Biophys. Acta 1062*, 94–102.

Rohrer, J., & Kuhn, A. (1990) *Science 250*, 1418–1421.

Roux, M., Neumann, J., Hodges, R. C., Devaux, P. F., & Bloom, M. (1989) *Biochemistry 28*, 2313–2321.

Sakmann, B., & Neher, E. (1983) *Single-Channel Recording*, Plenum Press, New York.

Sansom, M. S. P. (1991) *Prog. Biophys. Mol. Biol. 55*, 139–235.

Sansom, M. S. P. (1993) *Eur. Biophys. J. 22*, 105–124.

Schindler, H., & Quast, U. (1980) *Proc. Natl. Acad. Sci. U.S.A. 77*, 3052–3056.

Simon, S. M., & Blobel, G. (1992) *Cell 69*, 677–684.

Stankowski, S., Pawlak, M., Kaisheva, E., Robert, Ch. H., & Schwarz, G. (1991) *Biochim. Biophys. Acta 1069*, 77–86.

Thiaudière, E., Soekarjo, M., Kuchinka, E., Kuhn, A., & Vogel, H. (1993) *Biochemistry 32*, 12186–12196.

Tosteson, M. T., & Tosteson, D. C. (1981) *Biophys. J. 36*, 109–116.

Wolfe, R. B., Rice, M., & Wickner, W. (1985) *J. Biol. Chem. 260*, 1836–1841.